Available online at www.sciencedirect.com
ScienceDirect
Journal of the European Ceramic Society 31 (2011) 303–312
www.elsevier.com/locate/jeurceramsoc

Alumina foam catalyst supports for industrial steam reforming processes

Raphaël Faure [a,c,*], Fabrice Rossignol [a], Thierry Chartier [a], Claire Bonhomme [a], Alexandre Maître [a], Grégory Etchegoyen [b], Pascal Del Gallo [c], Daniel Gary [c]

[a] SPCTS, UMR 6638 CNRS-Université de Limoges, Centre Européen de la Céramique, 12 rue Atlantis, Limoges 87068, France
[b] CTTC, Limoges, France
[c] Air Liquide CRCD, Jouy-en-Josas, France

Received 9 July 2010; received in revised form 29 September 2010; accepted 2 October 2010
Available online 30 October 2010

Abstract

The manufacture and the characterisation of alumina foams as alternative catalysts supports for industrial steam reforming processes are presented here. The possibility of use of alumina foams as catalysts supports in such processes is evaluated by studying their resistance toward mechanical and chemical stresses. The alumina foams produced are characterised owing to their processing parameters (slurry infiltration, sintering temperature, template pore size). Their ability to work in hydrothermal atmosphere is assessed by characterising the evolution of microstructures and mechanical strengths upon aging. Thermodynamic studies of the stability of alumina in industrial steam reforming working conditions are performed and correlated to the experiments to demonstrate the stability of such a system.

Keywords: Shaping; Porous; Alumina foam; Catalyst support

1. Introduction

Ceramic foams are today widely used in technological applications, mainly in filtration (molten metal filters, hot gas filters). They are also considered for new applications in medicine (biomaterials, bone substitutes), in catalysis (catalyst supports) or in automotives (particulate filter for diesel engines). Ceramic foams are mainly processed by the replication technique, first described by Schwartzwalder and Somers.[1] It includes different steps: (i) the impregnation with ceramic slurry of reticulated templates having open porosities, (ii) the removal of the slurry excess to let the porosity open, (iii) the pyrolisis of the organics and (iv) the sintering of the ceramic body. Each step of the preparation has been widely studied and numerous publications can be found.[2–9]

In heterogeneous catalysis, the use of foam-supported catalysts is today in development in many processes such as pollution abatement processes (catalytic converters) or conventional catalytic processes,[8–10] including steam reforming (SR) processes.[11,12] Considering their high porosity and tortuosity, it has been found that foam supported catalysts are interesting for heat and mass transfer limited processes.

Steam reforming (SR) is a highly endothermic process used to produce H_2 or syngas (H_2/CO mixture in a 2 to 4.8 molar ratio) mainly by reacting water and methane.[13] This process produces today the major part of the hydrogen industrially used. Catalysts currently used are pellets, in the form of barrels (cylinders of approximately 2 cm in diameter and 2 cm in height, crossed in their height by 1 to 6 channels). This catalyst support is made of magnesium aluminate or calcium aluminate spinels (refractory materials, inert in SR reactions) and is prepared by extrusion or pressing. This support is then impregnated with metal precursors (mainly nickel) to provide the catalytic active phase. Catalysts are loaded in metallic tubes measuring 12 m height and 10–13 cm in diameter. Hundreds of vertical reforming tubes are located in furnaces heated by fuel or gas burners. Extremely severe working conditions are required to perform SR reactions: high temperatures (between 600 °C and 900 °C, as the reaction is highly endothermic), high pressures (20–30 bar) and mild atmospheres containing typically 1.5–3 mol of water per mole of reactant, depending on the reactant. Such process generally runs for several years in industrial units before a necessary change

* Corresponding author at: Air Liquide CRCD, 1 chemin de la Porte des Loges, Les Loges-en-Josas, 78354 Jouy-en-Josas, France.
E-mail addresses: raphael.faure@etu.unilim.fr, raphael.faure@airliquide.com (R. Faure), fabrice.rossignol@unilim.fr (F. Rossignol).

0955-2219/$ – see front matter © 2010 Elsevier Ltd. All rights reserved.
doi:10.1016/j.jeurceramsoc.2010.10.009

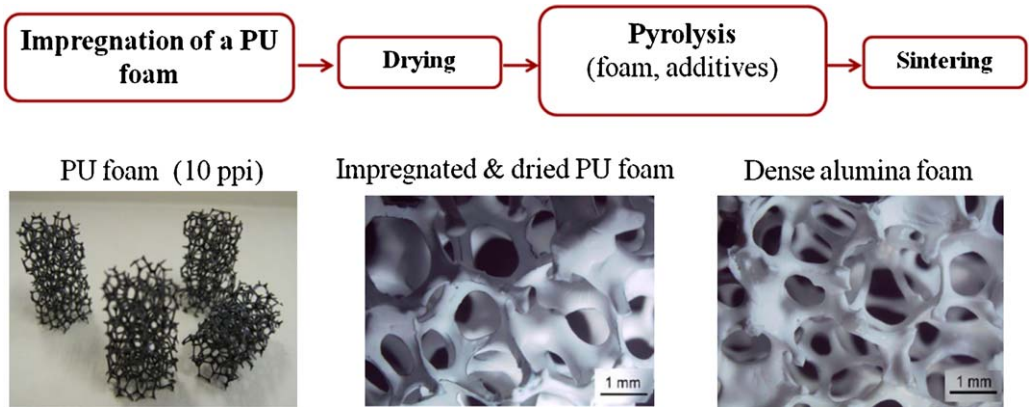

Fig. 1. Alumina foam preparation by slurry infiltration of PU templates.

of the catalytic load. The main issues currently encountered in SR industrial processes (tube cracks, corrosion by steam, catalyst deactivation/sintering by overheating, catalyst attrition), are directly related to the severe operating conditions. A direct drawback is a lowering of the life time of the reforming tubes, causing unexpected shut down of SR plants, with dramatic economical consequences. Barrel-shaped catalysts have proved to be efficient catalysts for SR processes as they are cheap, robust and efficient in producing syngas in good yields with high selectivity. However, barrel morphology when staked conducts to high pressure drops. Moreover stacking defects can appear if tubes are misfiled, leading to hot-spot formation that shorten the life-time of metallic tubes by crack formation.[14] Today, tubes are actually changed more often than the catalytic load itself. To overcome such issues, the use of alumina foams as monolithic catalyst supports for industrial SR processes is currently studied.

The advantages of monolithic supports over conventional powders or pelletized catalysts in heterogeneous catalysis are well established.[10,15] Monoliths are uni-body materials with a homogeneous and well-defined structure. Depending on their porosity size and design, they can possibly exhibit a low resistance to flow (e.g. low pressure drops). Among these monoliths, ceramic foam-supported catalysts present several advantages. Twigg[8,9,16] and Richardson[8,9,16–18] pointed out experimentally their beneficial effects in terms of pressure drop and heat/mass transfer. Hot spots are no longer observed because of the very limited number of stacking defects while filling the metallic tubes with near net shape foams. In addition, foams exhibit high surface to volume ratios and thus develop more exchange surfaces in a catalytic bed. Reaction kinetics is thus favoured.

However, the use of monolithic catalytic charges leads to new constraints. For instance, while stacking a column of 13 m of elemental foams of a height of 10 cm in an industrial tube, the foam at the bottom layer of the tube must resist to the mechanical stress imposed by the weight of the entire column above it. Moreover that mechanical strength might be affected by hydrothermal conditions, as alumina can react with water at elevated temperatures.[19–22] In this respect, this study essentially concern by corrosion (reaction of the gas phase with the support) and crushing of foams made of alumina.

Alumina has been chosen, as it has several advantages in comparison with other ceramic materials: it is inexpensive, quite highly refractory and supposed to be relatively inert with water in the range of pressure and temperatures of SR industrial processes (28–32 bar, 600–900 °C).

Although the interest of ceramic foams as catalyst supports is today well established, their stability against physical and chemical aggressions during in SR has never been discussed. In this study, the preparation and the characterisation of alumina foam supports are presented. The stability of the ceramic foams in hydrothermal atmosphere is first theoretically evaluated by thermodynamic modelling. Then, corrosion experiments are performed. These experiments are finally correlated to the evolution of mechanical strengths and microstructures.

2. Experimentals

2.1. Preparation of alumina foams

Alumina foams are prepared by impregnation of commercial polyester based polyurethane (PU) foams: 5 ppi (pore per inch) Calipore® foams from Caligen (Caligen Europ BV, Breda, Netherland) and 10 ppi, 20 ppi and 30 ppi Bulpren® S-type foams from Recticel (Recticel, Brussels, Belgium). Foams are cut into cylinders. Alumina slurries are prepared by dispersing commercial alumina CT3000SG® powders (Alcoa Industrial Chemicals, Pittsburg, USA) with 99.7% purity in water. Organic additives are used to stabilize the slurry, to favor the uniform coating of the template, to increase the adhesion of the slurry on the template or to prevent the blocking of the pores by formation of "windows".[5,6] Additives used are dispersing agents (ammonium polymethacrylate), binders (polyvinylacetates), wetting agents (octan-1-ol, docan-1-ol solution) and antifoaming agents (polyether siloxane). A block diagram describing the preparation process is presented Fig. 1. PU foams are impregnated by immersion in the slurry. The slurry is fluid enough to drain out of the template by gravity without any need of an additional driving force. The impregnation is repeated several times together with a drying in air at room temperature in between two successive impregnation steps. Using this approach, acceptable coverage rates are reached. Impregnated foams are then calcined in two steps. The first step consists in pyrolising the organic

additives and the PU template, and the second step corresponds to the sintering of the alumina body at 1600 °C for 1 h. Consolidated standard alumina foams thus obtained present hollow struts resulting from the PU template pyrolisis that may lower mechanical properties.

To strengthen these mechanical properties, a post-impregnation process has been developed by CTTC (CTTC, Limoges, France). The slurry used for the first set of impregnations described previously is twice diluted. The post-impregnation with that very fluid slurry allows to increase the struts diameter and to partly fill the holes in those struts. Post-impregnation is realized on ceramic foams that are pre-sintered at moderate temperature (1200 °C). Lower sintering temperature is required to maintain a residual porosity in alumina, in order to allow the slurry to enter the struts and to fill hollow struts. After post-impregnation, foams are sintered at 1600 °C for 1 h for consolidation.

2.2. Thermodynamic modelling and experimental measurements of corrosion

Thermodynamic modelling of the stability of alumina ceramics under water vapor and reducing gases are performed using GEMINI methodology.[23] It consists on a minimization of the total Gibbs energy of a multiconstituted and polyphased system under constant pressure conditions (equation), which leads to the thermochemical equilibrium of the system.

$$G = \sum_{i=1}^{\nu} x_i \mu_i \quad (1)$$

where x_i is the molar fraction of specie, μ_i is the chemical potential of i and ν corresponds to the number of chemical species.

Using COACH software (COmputer Aided CHemistry), an exhaustive thermodynamic database (heat capacity, enthalpy and entropy of formation, latent heat) of all possible gaseous species of our system, *i.e.* volatile aluminium hydroxides $Al(OH)_2$ and $Al(OH)_3$, is built.[24] Then, after GEMINI calculations, only gaseous species with a vapor partial pressure above 10^{-9} atm are considered to be relevant for corrosion.

Finally, the corrosion of alumina foams in steam is experimentally quantified by thermogravimetric analysis (TGA). It is assumed that observed weight losses can be attributed to volatilization of gaseous species (*e.g.* corrosion). TGA measurements are carried out using a Setsys apparatus (Setaram, Caluire, France) from room temperature to 1000 °C with heating and cooling rates of 5 °C/min and dwell time of 100 h at maximum temperature. A vapor generator (Wetsys) is used to control the relative humidity of the feed mixture: analyses are carried out in wet He (95% relative humidity). Bulk polished alumina samples are used here as it is required to both determine the surface modifications under vapor and to know the exact surface developed by the sample.

2.3. Aging of alumina foams

Alumina foams are hydrothermally aged in water rich atmosphere. The samples are submitted to flowing N_2/H_2O (1:3 molar ratio, 120 L h^{-1}) for 5 or 30 days, at 900 °C and at atmospheric pressure. Samples are introduced in an open alumina crucible in the furnace. The inner wall of the furnace is made of Ni-based metallic alloy resistant to corrosion in the working conditions. Before introduction in the tubular furnace the water is pre-heated at 300 °C and mixed with nitrogen. Then, the gas mixture is injected in the furnace heated at 900 °C. The composition of the atmosphere and the temperature of the treatment are chosen to be as representative as possible to SR atmosphere.

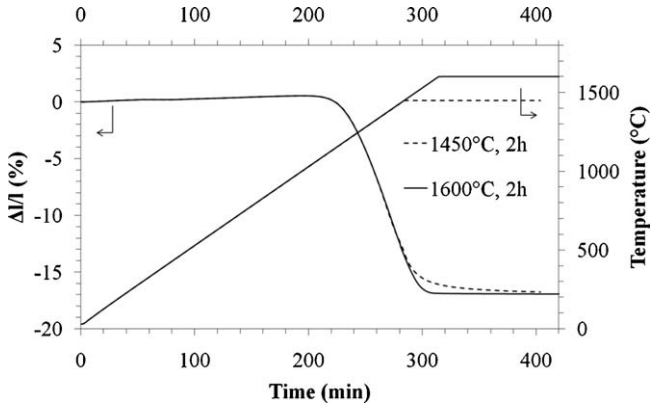

Fig. 2. Linear sintering shrinkage of a 10 ppi standard alumina foam for two different thermal treatments (1450 °C, 2 h or 1600 °C, 2 h).

2.4. Compressive strength measurements

The crush tests are performed on LR 50K Lloyd Instrument (Lloyd Instruments Ltd., Bognor Regis, UK) equipped with a 5 KN sensor. Compressive strengths are measured for fresh and aged foams. Tests performed on fresh foams are realized on cylindrical samples measuring 50 mm in height and 50 mm in diameter. Tests performed on aged foams are realized on samples measuring 32 mm in height and 40 mm in diameter.

2.5. Microstructural characterisation of alumina foams

A high-resolution scanning electron microscope equipped with a Field-Emission Gun (FEG-SEM), Jeol JSM-7400F (Jeol Ltd., Tokyo, Japan), is used to observe the microstructure of the surface and of the bulk of alumina foam struts before and after aging. Samples are prepared by attaching the foam struts to brass sample carriers with a silver paste. Bulk microstructures are observed after polishing and thermal etching at a temperature of 1550 °C for 15 min.

3. Results

3.1. Characterisation of alumina foams

Macroporous supports produced can exhibit different porosities. The pore size is directly linked to the template chosen for the impregnation, with additional 16–18% shrinkage due to sintering of alumina (Fig. 2). Alumina foams are labeled according the porosity of the template used, *i.e.* 10 ppi, 20 ppi or 30 ppi foams. A given foam (i) is also characterized by its density (ρ_i), its apparent porosity (φ_i) and its impregnation rate (τ_i). These

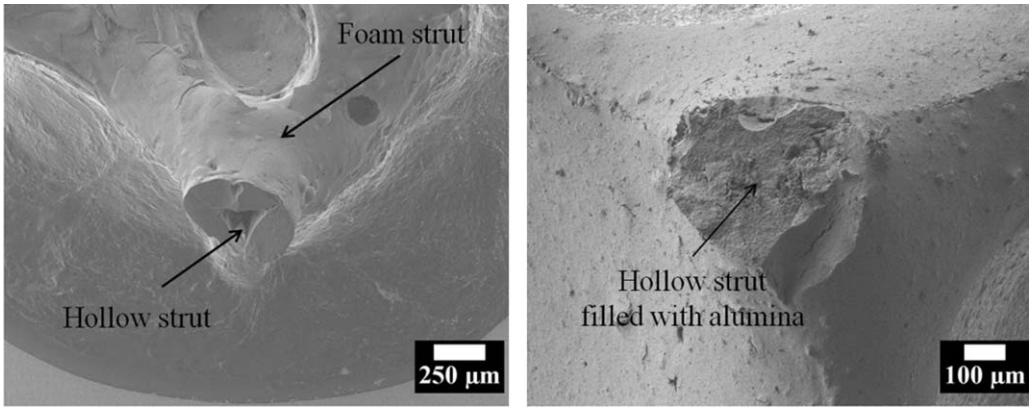

Fig. 3. Micrographs of foam struts after standard impregnation (A) and post-impregnations (B).

parameters are calculated as follows:

$$\rho_i = \frac{4m_i}{H_i \cdot \pi \cdot D_1^2} \quad (2)$$

$$\varphi_i = \frac{\rho_i}{\rho_{Al_2O_3}} \quad (3)$$

$$\tau_i = \frac{m_{imp}}{m_{imp} + m_{PU}} \quad (4)$$

with m_i the weight of alumina foam, m_{imp} the weight of dried impregnated PU foam, m_{PU} the weight of the PU foam template before impregnation, H_i the average height of the alumina foam and D_i its average diameter.

SEM micrographs of the core of standard and post-impregnated alumina foams struts are seen in Fig. 3. The advantages of the post-impregnation process over previously described techniques to strengthen foam struts clearly appear. In standard foams, hollow struts can be observed as expected (Fig. 3A). The hole is almost entirely filled in post-impregnated (Fig. 3B). Direct consequences are observed on the compressive strength of foams (Fig. 4C): crush strength values are at least doubled by post-impregnation.

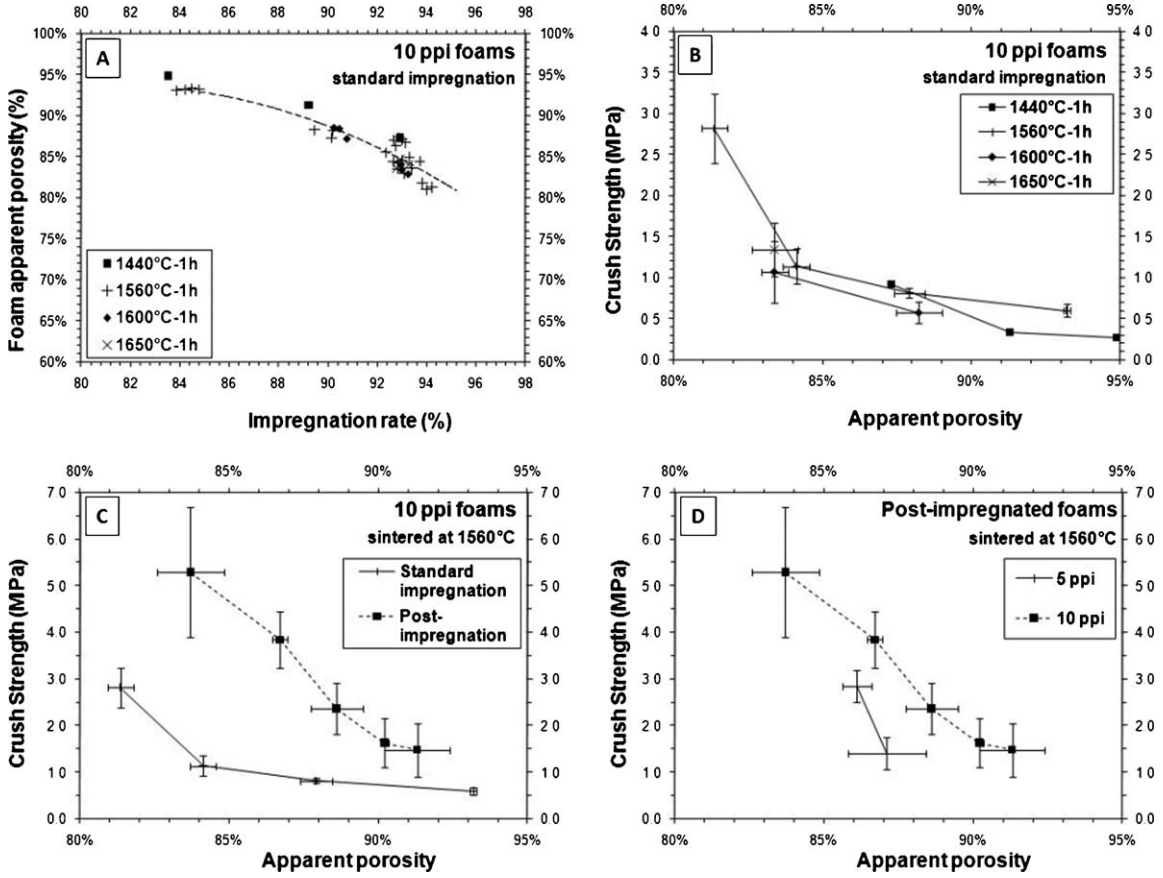

Fig. 4. (A) Influence of impregnation rate on apparent porosity. (B) Influence of apparent porosity and sintering temperature on crush strength. (C) Influence of apparent porosity and manufacturing process on crush strength. (D) Influence of apparent porosity and pore size on crush strength.

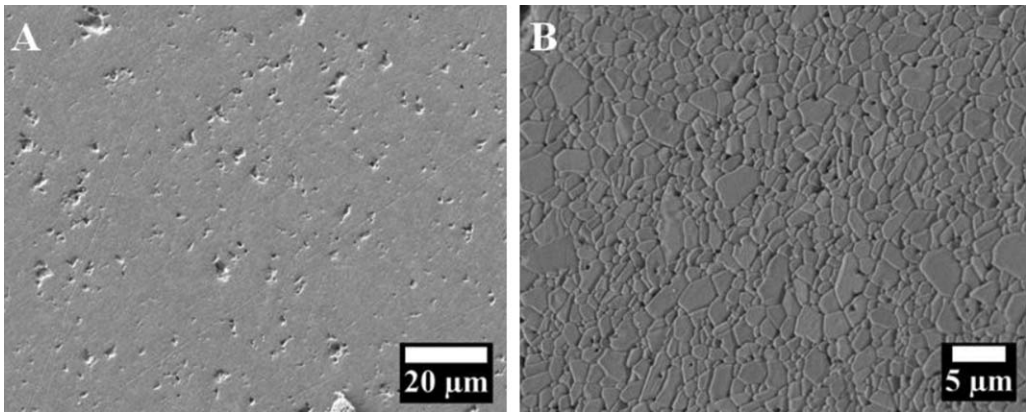

Fig. 5. Microstructure of the core of foam struts sintered at 1600 °C for 1 h. (A) Polished surface; (B) polished and thermally etched surface.

Moreover, the apparent porosity of the foams can be tailored by adjusting the impregnation rate (Eq. (4)) during the preparation (Fig. 4A). Since the average diameter of foam struts increases when increasing the impregnation rate, its compressive strength also increases.

SEM images of the foam microstructures, similar to Fig. 4.

A and B, are used to quantify grain size and densification by image analysis (ImageJ software). The relative density ranges from 98.5% to 99.5% (Fig. 5A). The average grain size (d_{50}) of alumina sintered at 1600 °C for 1 h foams is 1.3 ± 0.2 µm (Fig. 5B).

Compressive strength has been evaluated for foams of different pore sizes (5 ppi, 10 ppi, Fig. 4D), of different apparent porosity (82–94%) and different sintering temperatures (1440–1650 °C, Fig. 4 B). The consequence of the manufacturing process on compressive strength, *i.e.* standard or post-impregnation, is also evaluated (Fig. 4C).

For a given apparent porosity, almost no variation of the crush strength is measured in the tested sintering temperature range (1440–1650 °C, Fig. 4B). It means that the consolidation of struts at 1440 °C is sufficient enough and not the limiting parameter controlling the rupture, in accordance with the similar densification rates observed (Fig. 2) for two different sintering temperatures (1450 °C and 1600 °C). The rupture is actually controlled by two parameters: (i) the macroscopic nature of the foam itself (ppi level) and (ii) the thickness of elementary struts. Concerning the thickness of struts, for a given ppi level, the higher that thickness is (*i.e.* high impregnation rate, low apparent porosity), the larger the surface submitted to a given load, and thus the lower the stress. Concerning the ppi level, for a given apparent porosity, the larger the macropores are (*i.e.* low ppi level), the lower the crush strength (Fig. 4D): crush strength for 5 ppi and 10 ppi alumina foams are 1.4 MPa and 2.5–3 MPa respectively, with apparent porosities in a similar range (around 87%) to allow comparison. It has to be noticed that a part of the strength loss might also be attributed to the fact that 5 ppi PU templates exhibit larger foam struts than 10 ppi templates. Consequently the hollow ceramic struts formed by pyrolisis are larger for 5 ppi foams.

3.2. Tailored alumina foams architecture

In steam reforming processes such as in steam methane reforming (SMR), the reaction requires heat to proceed as it is highly endothermic. Since the current SR processes use homogeneously heated SR tubes, thermal gradients appear between the top part and the bottom part of the catalytic bed, as reactants consumes heat. In order to limit the consequence of the endothermicity of the steam reforming reaction in terms of temperature gradients, it has been thought that it could be interesting to control the amount of active phase (*i.e.* the part of the catalyst responsible for the control of the reaction kinetics) deposited on the alumina foam support. In such a system, the active phase is deposited on the alumina foam struts: the smaller the porosity of the foam, the higher the surface per volume ratio, the higher the catalyst loading. As the heat consumed by the reaction is linked to the number of active sites per volume unit of catalyst, the control of the porosity can be a crucial parameter to control the thermal gradient. Since we can decrease the number of active sites in the top part of the catalytic bed, it is possible to decrease the amount of heat consumed in the top part of the reactor, and thus to extend the endothermic event along the catalytic bed.

Based on methods described in the literature for production of ceramic foams with porosity gradients,[25–27] we have then produced original alumina foams with tailored architectures regarding the SR process requirements in terms of temperature gradients. These original alumina foams exhibit longitudinal and/or radial porosity gradients (Figs. 6 and 7). Their application in SR processes is currently evaluated.[28–30]

3.3. Stability of alumina foams in hydrothermal atmosphere

3.3.1. Thermodynamic predictions

All calculations are carried out in isothermal and isobar conditions, in the 650–1800 °C temperature range. The solid phase is chosen in large excess (100:1 in molar ratio) compared to the gaseous species (CH_4, H_2O) to avoid its complete consumption.

The main gas species participating to the SR reaction are methane, which initial partial pressures of 7 and 21 atm.

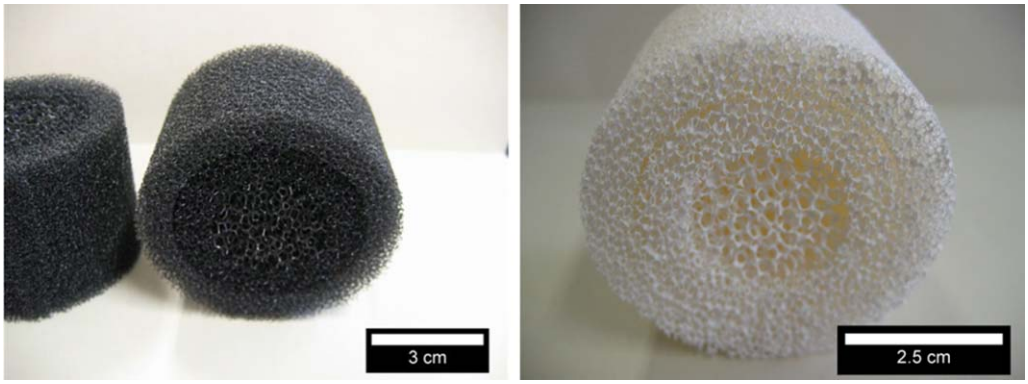

Fig. 6. PU foams (left) and as-obtained alumina foams (right) with discontinuous radial porosity gradients.

Alumina is thermodynamically stable under reforming conditions up to 950 °C (Fig. 8). At this temperature, low partial pressures of 2.75×10^{-8} atm of gaseous aluminum hydroxides $Al(OH)_3$ and $Al(OH)_2$ are formed, which is not significant. $Al(OH)_2$ is the predominant hydroxide since the Al^{II} is more stable than Al^{III} in reducing atmospheres (Table 1). The Al_2O_3 solid phase begins to be unstable from 1450 °C, with formation of a significant amount of aluminum hydroxides. Since the SR process is working between 650 °C and 900 °C, such a corrosion effect should not be observed in SR reactors. Alumina is thus considered to be thermodynamically stable in SR atmospheres.

3.3.2. *Experimental characterization of the alumina foam hydrothermal stability*

The thermodynamic results have been correlated to experimental measurements. At 1000 °C, the thermodynamic data have established that alumina does not react with water at the equilibrium. The weight variations in steam at 1000 °C have been measured during 100 h dwell time, to confirm those thermodynamic results (Fig. 9). No variations can be observed at this temperature. It is thus considered that our alumina foams are stable upon aging in water-rich atmosphere at 1000 °C.

3.4. *Alumina foams microstructure and mechanical properties upon aging*

Alumina foams have been aged at 900 °C, for different length times (5 days, 30 days) in a water-rich atmosphere (H_2O/N_2 3:1 in molar ratio). The surface and the core of alumina foams have been observed before and after aging. The initial microstructure of the surface of alumina foams exhibits facetted alumina particles with well-defined edges (Fig. 10A). No changes are observed after 2 days of aging treatment (Fig. 10B). However, after 30 days, the surface of the foam appears slightly modified,

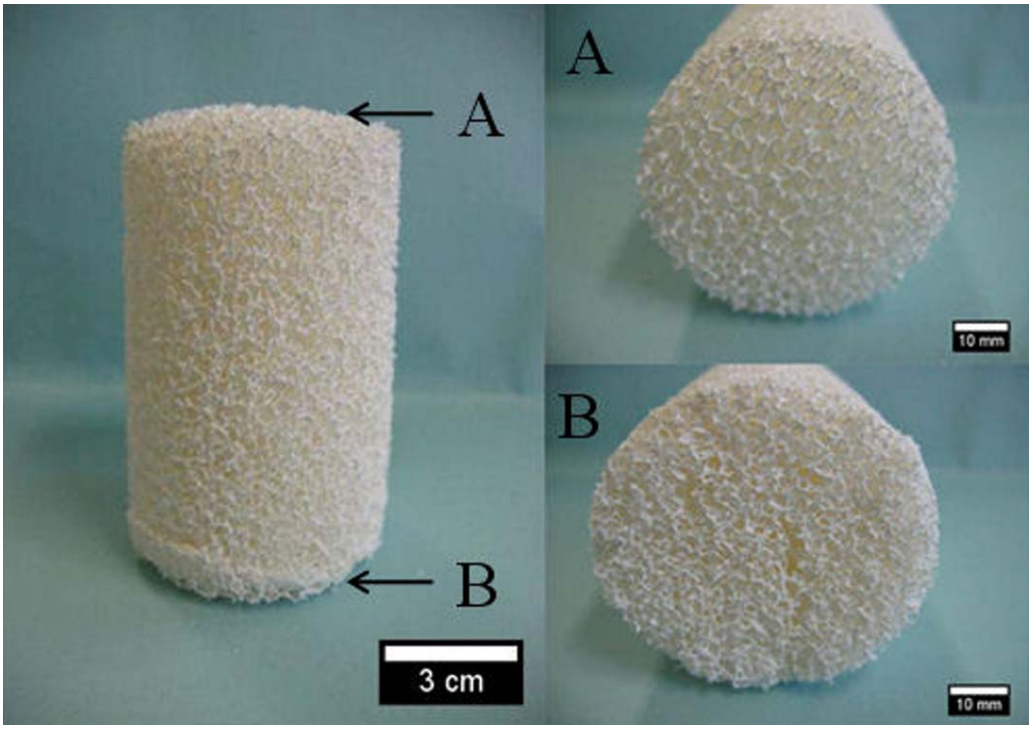

Fig. 7. Alumina foam with longitudinal continuous porosity gradient.

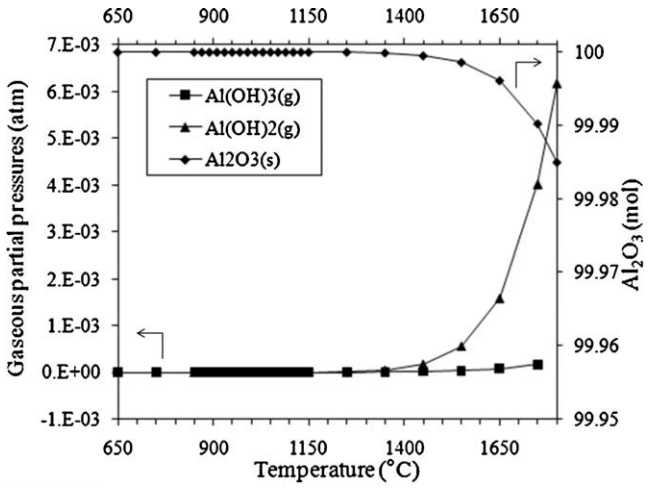

Fig. 8. Thermodynamic evolution of the Al_2O_3 solid phase and $Al(OH)_3$/$Al(OH)_2$ gaseous phases at elevated temperature in a mixed atmosphere CH_4/H_2O 1:3, under 31 bar.

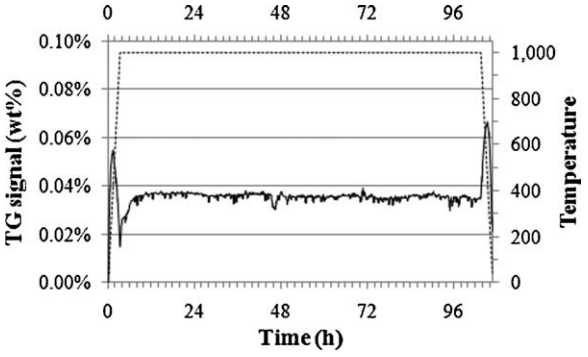

Fig. 9. TGA analysis of alumina foam in water-rich atmosphere.

the grain facets being less marked (Fig. 10C). Moreover nano-sized particles with a diameter of 30–50 nm are observed at the grain boundaries (Fig. 10D). Those tiny particles are assumed to be contaminants traces present in the water, mainly salts, accumulated during 30 days of aging treatment.

On the contrary, no effect of aging is observed in the bulk. After 2 days and 30 days, microstructure similar to that presented in Fig. 5B is retained.

To confirm direct observations, compressive crush strength measurements have been performed on alumina foams initially aged for 5 days at 900 °C in a water-rich atmosphere (Fig. 11). The results are compared to foams with exactly the same size but without aging treatment from a different fabrication batch which explains the slight difference in terms of apparent porosity (Fig. 4). Obviously, there is no change of the mechanical properties of foams upon aging as expected regarding the thermodynamic stability of alumina.

4. Discussions

4.1. Advantages of the use of foams in catalysis

The performances of alumina foams produced are currently tested in terms of pressure drops and temperature gradients in pilot tests. Although the benefits of such foam catalyst supports have been outlined in the literature, only a few applications have been developed at the industrial scale.[8,9,11,12,17,18] Since foams are highly porous (porosity ranging from 80% to 95%), they create lower pressure drops than pellets, developing at the same time equivalent or higher geometric surface area.[17] The pressure drop through foams increases when decreasing the pore size. Elevated porosity make foams preferential supports for heat and mass transfer limited processes.[18] Twigg and Richardson provide a list of reactions for which foam catalyst supports can be useful.[8] Higher turn-over frequencies have been reached by the use of foams, in comparison to pellets, in dry reforming of methane.[31] Interesting results from patents are reported in references[11,12] for steam reforming applications. Usually reforming tubes of 12 m length are required to attain the thermodynamic equilibrium of the SMR reaction. The typical temperature gradient observed in industrial SMR reactions is represented in Fig. 12. It has been claimed that with foams SMR reaction can be performed within one-half of the reforming tube, and that temperature gradient in the front of the tube appeared considerably reduced.

Table 1
Thermodynamic evolution of the feed composition and of the alumina support in SMR-like conditions.

Temperature (°C)	Feed mixture (atm)						Catalyst support evolution		
	H_2O	H_2	CH_4	CO_2	CO	N_2	Al_2O_3 (mol)	$Al(OH)_2$ (atm)	$Al(OH)_3$ (atm)
650	16.2	7.8	4.6	1.8	0.4	0.1	1.0000E+02	0.00E+00	0.00E+00
750	13.3	11.3	3.0	2.0	1.3	0.1	1.0000E+02	0.00E+00	0.00E+00
850	10.8	14.3	1.4	1.8	2.6	0.1	1.0000E+02	0.00E+00	0.00E+00
950	9.5	15.9	0.4	1.5	3.6	0.1	1.0000E+02	2.75E−08	0.00E+00
1050	9.2	16.3	0.1	1.2	4.0	0.1	1.0000E+02	2.79E−07	1.16E−07
1150	9.3	16.3	0.0	1.1	4.2	0.1	1.0000E+02	1.97E−06	5.09E−07
1250	9.4	16.2	0.0	0.9	4.3	0.1	1.0000E+02	1.08E−05	1.84E−06
1350	9.5	16.1	0.0	0.8	4.4	0.1	1.0000E+02	4.76E−05	5.70E−06
1450	9.5	16.1	0.0	0.8	4.5	0.1	1.0000E+02	1.76E−04	1.54E−05
1550	9.6	16.0	0.0	0.7	4.6	0.1	9.9999E+01	5.62E−04	3.72E−05
1650	9.7	16.0	0.0	0.7	4.6	0.1	9.9996E+01	1.58E−03	8.17E−05
1750	9.7	15.9	0.0	0.6	4.7	0.1	9.9990E+01	4.02E−03	1.65E−04
1800	9.7	15.9	0.0	0.6	4.7	0.1	9.9985E+01	6.18E−03	2.29E−04

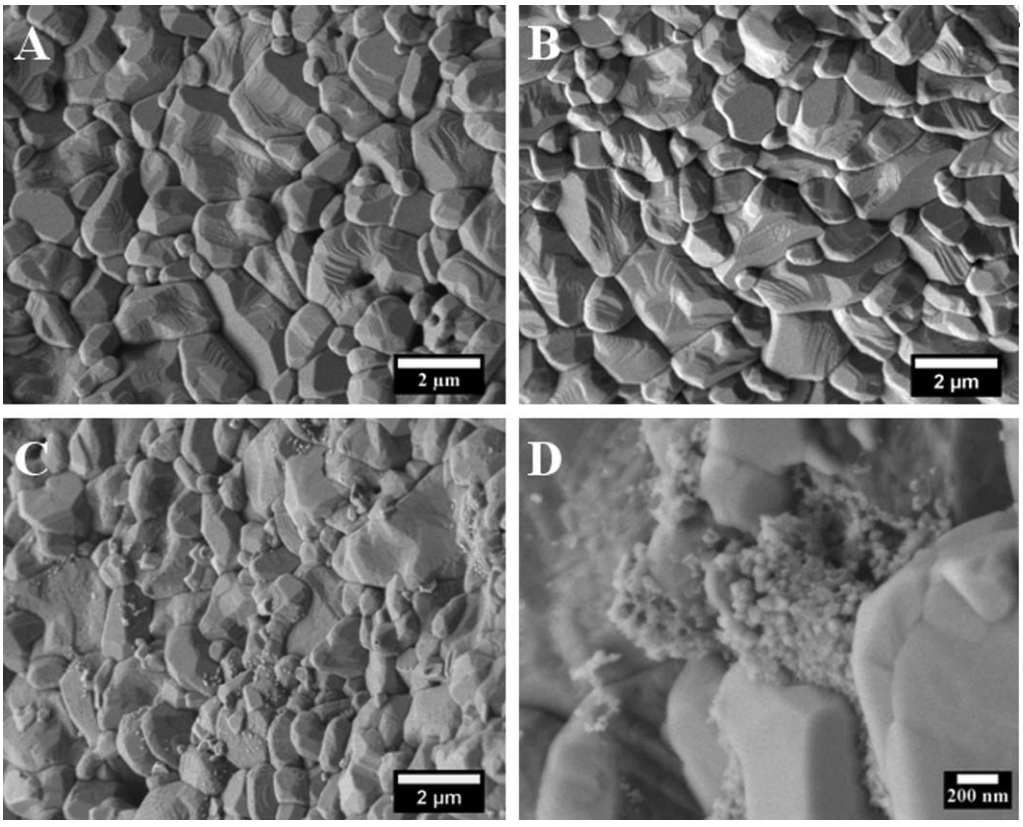

Fig. 10. Microstructure of the alumina foam surface before aging (A) and after 5 days (B) and 30 days (C and D) of aging treatment in water rich atmosphere at 900 °C.

In addition to the higher porosity and tortuosity of foams over pellets, barrels and other catalyst supports, graded catalytic beds have been successfully used to increase the control of the temperature for heat limited processes (highly endothermic or exothermic) in industrial reactors.[32–37] Various temperature profiles can be obtained by diluting the catalytic bed with inert materials.[32] It is therefore also established that the dilution with inert material can affect the conversion rate of the reaction.[37] The principle of dilution is to locally decrease in the reactor the density of active sites by introducing inert materials such as quartz or corundum. Consequently, the reaction is more homogeneously distributed along the reactor and not only in the feeding region. The optimum thermal profile for a reaction can be obtained by varying the ratio of inert material/catalyst along the catalytic bed, or by using dilutants of different sizes.[33]

Foams as catalyst supports are interesting alternatives to the use of dilutants. Foams can be produced in various shapes and sizes, according to the process concerned, by simply modifying the template used for their fabrication. Furthermore ceramic foams showing porosity gradients have been developed. They allow to control the amount of active phase along the catalytic bed of the reactor.[28–30] Porosity gradients can also be achieved simply by stacking foam monoliths with different porosity.

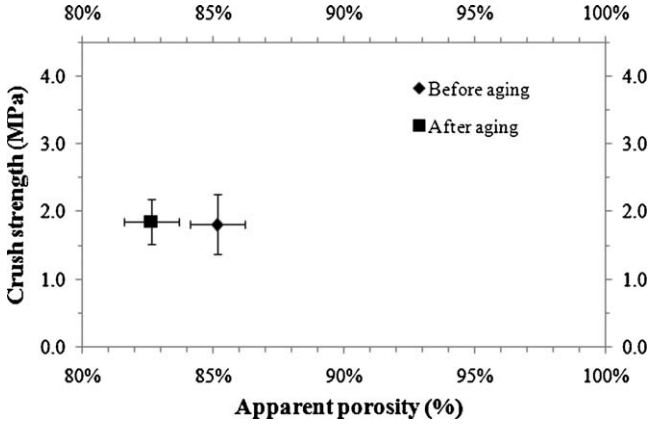

Fig. 11. Crush strengths of alumina foams before and after 5 days aging in hydrothermal atmosphere.

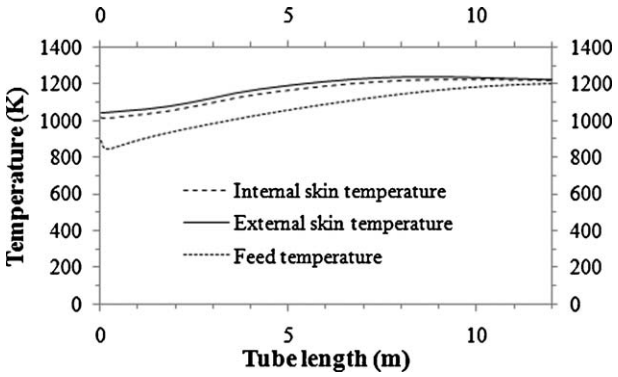

Fig. 12. Typical temperature profile in SMR tubes.

4.2. Alumina foams upon aging

Since alumina foams are used in industrial processes, the safety levels requirements are high. In addition to the risks, the cost of unit shutdown is dramatically elevated. In SR processes, foams must keep their integrity at elevated temperatures and pressures, and with respect to the nature of the hydrothermal atmosphere which is highly reductive (CH_4, H_2) and corrosive (CO, H_2). Water is known to favour materials transport. Moreover, one key feature of foams *vs.* conventional barrels is that damaging by attrition (friction between pellets) does not occur. Finally, the density of foams (0.4–0.7 g cm^{-3}) is much lower than that of barrels (1.3–1.6 g cm^{-3}), thus leading to a lower compressive stress on the catalytic charge. The maximum acceptable compressive stress value at the bottom of the catalytic bed can be calculated considering tubular reactors of 12 m height and 10 cm diameter, filled with 60 kg of alumina foams showing 85% porosity (*i.e.* a density of 600 kg m^{-3}). The maximum acceptable compressive stress is estimated by reporting the weight of the foam stacking to the section of a tube (0.008 m^2): it is estimated to be around 0.75 MPa for foams of 10 cm diameter. After a post-impregnation process (Fig. 4) followed by aging (Fig. 11), the compressive stresses measured (around 4 MPa) exceed the required value.

Corrosion mechanisms of alumina in water vapour atmosphere have not yet been fully investigated in the literature. Experiments realised by Opila and Myers show that volatilisation can occur by formation of $Al(OH)_3$ gaseous compounds following Eq. (5), in flowing water vapour atmosphere, leading to weight losses.[20]

$$Al_2O_3(s) + 3H_2O_{(g)} = 2Al(OH)_{3(g)}$$
$$\Delta H = 210 \pm 20\,\text{kJ mol}^{-1} \quad (5)$$

The previous authors also show that this compound is present but in negligible amounts at 1250 °C, for water partial pressure ranging between 0.15 and 0.68 atm. In static atmosphere, corrosion phenomenon is observed at higher temperatures. That corrosion is accompanied by a weight increase although there is volatilisation of $Al(OH)_3$.[22] The modification of the lattice parameters together with that weight increase is explained by insertion of water in the hexagonal structure of alumina. Both water uptake (weight gain) and $Al(OH)_3$ volatilisation (weight loss) are assumed to be responsible for corrosion. In any cases (flowing or static atmosphere), surface rearrangement faceting the grains is observed, coupled with grain coarsening.[20–22] Such a phenomenon is an experimental evidence of alumina volatilisation. To our knowledge, no data is found on the hydrothermal stability of alumina between 600 °C and 900 °C, even though volatilisation of alumina should not be a problem below 1000 °C. However, grain coarsening could dramatically decrease the mechanical strength of monoliths.

In the present study, such issues are not observed for alumina foams in the temperature range of interest for SR. In fact, no changes in the bulk microstructure and in crush tests performed before and after aging are observed. In addition, thermodynamic predictions (Fig. 8, Table 1) and TGA measurements (Fig. 9) in the temperature range 650–1800 °C both attest of the stability of alumina in water-rich atmosphere. However a low surface corrosion is observed after long term aging (Fig. 10C and D). It might be the result of a surface migration of alumina. We have confirmed such a phenomenon on polished samples aged in air and in a water-rich atmosphere (H_2O/N_2 3:1 in molar ratio) at 900 °C for 5 days. The surface of aged samples shows different microstructures depending on the nature of the aging atmosphere. Before any aging treatment, the grain boundaries are not visible on the alumina surface. No changes are observed after aging in air, whereas grain boundaries are etched after aging in water-rich atmosphere (Fig. 13). Impurities of commercial alumina, such as SiO_2 (0.03%), Na_2O (0.08%), CaO (0.02%), Fe_2O_3 (0.02%) and MgO (0.09%), are mainly located at the grain boundaries. Water vapour increases the mobility of these oxides at grain boundaries (Fig. 10D), which are either volatilised or moved from grain boundaries into a thermodynamically more stable configuration.

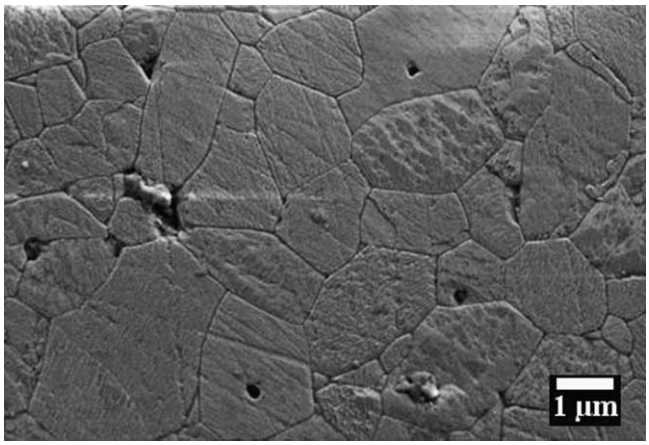

Fig. 13. Higher magnification of polished surfaces of alumina foam struts after aging in water rich atmosphere.

5. Conclusion

Foams are today considered as potential catalyst supports. The use of ceramic materials to manufacture foams is advantageous in processes requiring stability at high temperatures and under corrosive atmospheres. Alumina foams obtained by impregnation of sponge-like PU templates have been prepared by single or post-impregnation procedure. The resistance to compressive stresses has been increased by post-impregnation. The thermodynamic stability of alumina in a water-rich atmosphere has been evaluated through thermodynamic calculations. Negligible amounts of volatile aluminum hydroxides can be formed in the temperature range of interest for SR reactions, even though water is shown to cause limited corrosion of the surface at grain boundaries upon long lasting aging treatments. However, this corrosion phenomenon is only limited to the surface. The influence of aging in water-rich atmospheres on the resistance of foams to compressive stresses has been evaluated. It has been shown that aging treatment does not affect that resistance.

Foams produced exhibit different pore sizes, with porosity gradients enabling to control the active phase concentration in the catalytic bed. Traditionally, the use of graded active phase concentration is a solution to control the temperature in exothermic and endothermic processes. Foams with porosity gradients are then interesting alternatives to graded catalytic beds.

Acknowledgements

This study was realised in the framework of the FUI-BioH2Gen project managed by Air Liquide and supported financially by the French Ministry of Industry and the Limousin Regional Council.

References

1. Schwartzwalder K, Somers AV. *Method of making porous ceramic articles*. United States Patent Office 3,090,094; 1963.
2. Colombo P. Conventional and novel processing methods for cellular ceramics. *Philosophical Transactions: Mathematical, Physical and Engineering Sciences (Series A)* 2006;**364**(1838):109–24.
3. Lange FF, Miller KT. Open cell, low density ceramics fabricated from reticulated polymer substrates. *Advanced Ceramic Materials* 1987;**2**(4):827–31.
4. Luyten J, Thijs I, Vandermeulen W, Mullens S, Wallaeys B, Mortelmans R. Strong ceramic foams from polyurethane templates. *Advances in Applied Ceramics* 2005;**104**(1):4–8.
5. Montanaro L, Jorand Y, Fantozzi G, Negro A. Ceramic foams by powder processing. *Journal of the European Ceramic Society* 1998;**18**(9):1339–50.
6. Saggio-Woyansky J, Scott CE. Processing of porous ceramics. *American Ceramic Society Bulletin* 1992;**71**(11):1674–82.
7. Studart AR, Gonzenbach UT, Tervoort E, Gauckler LJ. Processing routes to macroporous ceramics: a review. *Journal of the American Ceramic Society* 2006;**89**(6):1771–89.
8. Twigg MV, Richardson JT. Theory and applications of ceramic foam catalysts. *Chemical Engineering Research and Design* 2002;**80**(2):183–9.
9. Twigg MV, Richardson JT. Fundamentals and applications of structured ceramic foam catalysts. *Industrial and Engineering Chemistry Research* 2007;**46**(12):4166–77.
10. Heck RM, Gulati S, Farrauto RJ. The application of monoliths for gas phase catalytic reactions. *Chemical Engineering Journal* 2001;**82**(1–3):149–56.
11. Twigg MV, Sengelow WM. *Foam catalysts, method of manufacture and method of using*. US Patent 4,810.685; 1989.
12. Twigg MV, Sengelow WM. *Catalysts for reforming hydrocarbon feedstocks*. US Patent 4.863,712; 1989.
13. Bartholomew CH, Farrauto RJ. *Fundamentals of industrial catalytic processes. Chapter 6: hydrogen production and synthesis gas reactions*. 2nd ed. Wiley–Interscience; 2006. p. 342.
14. High precision catalyst loading. *Nitrogen + Syngas* 2009;July–August (no. 300):7–41.
15. Farrauto R, Liu Y, Ruettinger W, Ilinich O, Shore L, Giroux T. Precious metal catalysts supported on ceramic and metal monolithic structures for the hydrogen economy. *Catalysis Reviews – Science and Engineering* 2007;**49**(2):141–96.
16. Twigg MV, Richardson JT. Structured ceramic foams as catalyst supports for highly exothermic processes. In: Gaigneaux EM, Devillers M, Hermans S, Ruiz P, Vos DE, Jacobs PA, Martens JA, editors. *Studies in surface science and catalysis*, 162. 2006. p. 135–42.
17. Richardson JT, Peng Y, Remue D. Properties of ceramic foam catalyst supports: pressure drop. *Applied Catalysis A: General* 2000;**204**(1):19–32.
18. Richardson JT, Remue D, Hung JK. Properties of ceramic foam catalyst supports: mass and heat transfer. *Applied Catalysis A: General* 2003;**250**(2):319–29.
19. Opila EJ, Jacobson NS, Myers DL, Copland EH. Predicting oxide stability in high-temperature water vapor. *JOM* 2006;**58**(1):22–8.
20. Opila EJ, Myers DL. Alumina volatility in water vapor at elevated temperatures. *Journal of the American Ceramic Society* 2004;**87**(9):1701–5.
21. Tai WP, Watanabe T, Jacobson NS. High-temperature stability of alumina in argon and argon/water-vapor environments. *Journal of the American Ceramic Society* 1999;**82**(1):245–8.
22. Ueno S, Jayaseelan DD, Kondo N, Ohji T, Kanzaki S. Corrosion behavior of Al_2O_3 in static state water vapor environment at high temperature. *Journal of Materials Science* 2004;**39**(21):6627–9.
23. GEMINI. *Thermochemical Scientific Software, Thermodata, INPG, CNRS*; 2003.
24. COACH. *Thermochemical Databank Software, Thermodata, INPG, CNRS*; 2003.
25. Cichocki Jr FR, Trumble KP, Rödel J. Tailored porosity gradients via colloidal infiltration of compression-molded sponges. *Journal of the American Ceramic Society* 1998;**81**(6):1661–4.
26. Hsu YH, Turner IG, Miles AW. Fabrication of porous bioceramics with porosity gradients similar to the bimodal structure of cortical and cancellous bone. *Journal of Materials Science: Materials in Medicine* 2007;**18**(12):2251–6.
27. Hsu YH, Turner IG, Miles AW. Techniques for manufacturing FGM bioceramics. *Key Engineering Materials* 2008;**361–363**(I):123–6.
28. Del Gallo P, Chartier T, Cornillac M, Faure R, Gary D, Rossignol F. *Ceramic foams with gradients of composition in heterogeneous catalysis*. EPO EP 2,141,139 A1; 2010.
29. Del Gallo P, Cornillac M, Rossignol F, Faure R, Chartier T, Gary D. *Ceramic foams with gradient of porosity in heterogeneous catalysis*. EPO EP 2,123,618 A1; 2010.
30. Del Gallo P, Gary D, Chartier T, Cornillac M, Faure R, Rossignol F. *Ceramic foams with gradient of porosity and gradient of catalytic active(s) phase(s)*. EPO EP 2,141,140 A1; 2010.
31. Peng Y, Richardson JT. Properties of ceramic foam catalyst supports: one-dimensional and two-dimensional heat transfer correlations. *Applied Catalysis A: General* 2004;**266**(2):235–44.
32. Caldwell AD, Calderbank PH. Catalyst dilution. A: means of temperature control in packed tubular reactors. *British Chemical Engineering* 1969;**14**(9):1199–201.
33. Hwang S, Linke P, Smith R. Heterogeneous catalytic reactor design with optimum temperature profile. II: application of non-uniform catalyst. *Chemical Engineering Science* 2004;**59**(20):4245–60.
34. Hwang S, Smith R. Heterogeneous catalytic reactor design with optimum temperature profile. I: application of catalyst dilution and side-stream distribution. *Chemical Engineering Science* 2004;**59**(20):4229–43.
35. Rajasree R, Ravi Kumar V, Dattatraya Kulkarni B. Performance enhancement of steam methane reforming using tubular packed-bed microreactors and dilution by adsorbent. *Energy and Fuels* 2006;**20**(2):463–72.
36. Taniewski M, Lachowicz A, Skutil K, Czechowicz D. The effect of dilution of the catalyst bed on its heat-transfer characteristics in oxidative coupling of methane. *Chemical Engineering Science* 1996;**51**(18):4271–8.
37. Van Den Bleek CM, Van Der Wiele K, Van Den Berg PJ. The effect of dilution on the degree of conversion in fixed bed catalytic reactors. *Chemical Engineering Science* 1969;**24**(4):681–94.